Changes in the Shadow: The Shifting Role of Shaded Leaves in Global Carbon and Water Cycles Under Climate Change

Liming He, Jing M. Chen, Alemu Gonsamo, Xiangzhong Luo, Rong Wang, Yang Liu, and Ronggao Liu

Abstract

Globally shaded leaves contribute to more than a half of the total increase in gross primary production (GPP; 7.6 Pg C) for 1982–2016. During 1982–2016, the fraction of shaded GPP increases by 1.1% ($p < 0.01$) in tropical forests and decreases by 1.4% ($p < 0.01$) and 1.8% ($p < 0.01$) in evergreen needleleaf and deciduous needleleaf boreal forests, respectively, suggesting an ecological niche of certain canopy structure for ecosystems to achieve maximum GPP. Unlike transpiration from sunlit leaves that has a turning point in the trend in 2003, global transpiration from shaded leaves steadily increased at the rate of 34 km^3/year ($p < 0.0001$) during 1982–2016. Our study therefore suggests that shaded leaves have an increasing role in buffering the adverse impact of climate change and extremes. Further studies are still needed to reduce the uncertainties in reported trends arisen from climate forcing data, leaf area index, and land cover and land change products.

1 Introduction

In 1982 to 2016, the global land surface air temperature has increased by 0.79 °C (Goddard Institute for Space Studies Surface Temperature Analysis, 2017; Hansen et al., 2010). The warming trend continues with large uncertainties associated to human's commitment to reduce carbon emission (Millar et al., 2017). Global warming with CO_2 fertilization (Drake et al., 2017), regional increase of droughts and heatwaves (Mazdiyasni & AghaKouchak, 2015; Williams, 2014; Zhang, Xiao, et al., 2016), and aerosol emissions (Landry et al., 2017; Lu et al., 2017) have led to significant impacts on terrestrial ecosystem's structure, function, and evolution (Maestre et al., 2016; McCluney et al., 2012; Pecl et al., 2017; Soliveres et al., 2015; Vazquez et al., 2017). Plant photosynthesis and transpiration are primary functions of an ecosystem, and their variations at different spatio-temporal scales are needed to understand the impacts of climate change on terrestrial ecosystems.

Carbon (C) assimilation through photosynthesis is tightly coupled with transpiration through stomata at the leaf level (Wolz et al., 2017). Radiation, ambient air temperature, and transpiration together determine leaf temperature, which in turn affects the leaf photosynthetic capacity through altered carboxylation rate. The sunlit portion of a canopy receives both direct and diffuse radiation, while shaded leaves receive only diffuse radiation for photosynthesis; therefore, the temperature of shaded leaves is usually a few degrees lower than that of sunlit leaves (Spayd et al., 2002). Systemic change in leaf temperature can significantly affect the C assimilation and

transpiration (Amissah et al., 2015; Martins et al., 2014; Quero et al., 2006). For example, shading a canopy from the Sun was found to be effective for photoinhibition mitigation and water use efficiency (WUE) improvement (Alarcon et al., 2006; Montanaro et al., 2009; Sofo et al., 2009). Rising temperature leads to increases in stomatal conductance and transpiration, which in turn may result in reduction of leaf temperature (Urban et al., 2017a, 2017b). Due to the complexity of canopy structure (Ashton & Berlyn, 1992; de Casas et al., 2011; Keenan & Niinemets, 2016; Valladares et al., 2016), it is expected that the same climate change may cause opposite consequences to the shaded and sunlit parts of an ecosystem, depending on the location of biomes and structure of a canopy (supporting information, Figure S1).

Advanced ecosystem models separate the calculation of C assimilation and transpiration for sunlit and shaded leaves (Bonan et al., 2014; Chen et al., 1999; Dai et al., 2004; Jiang & Ryu, 2016), assuming that a canopy is stratified into representative sunlit and shaded leaf groups. For each group, a leaf-level photosynthesis model is used to calculate the coupled C and water fluxes (Ball et al., 1987; Farquhar et al., 1980). The canopy-level flux is then taken as the total fluxes from sunlit and shaded leaf groups. The separation of C and water fluxes into their sunlit and shaded components enables us to diagnose the nonlinear effects of climate change on global C and water cycles (Chen et al., 2012, 2016; Mao et al., 2015; Zhang, Peña-Arancibia, et al., 2016). Stratification of canopy into two or more layers optimizes the modeling of carbon-water coupling for improving fluxes estimation (Luo et al., 2018). For example, a multilayer model was used to find the optimal canopy structure to achieve maximum crop productivity without change in water use or albedo (Drewry et al., 2014).

Although a great number of global estimates of the two largest fluxes in terrestrial ecosystems, gross primary production (GPP) and evapotranspiration (ET), are currently available, they do not converge on spatial distributions nor in long-term trends (Anav et al., 2015; Beer et al., 2010; Chen et al., 2017; He, Chen, Liu, et al., 2017; He, Chen, Croft, et al., 2017; Jiang & Ryu, 2016; Jung et al., 2010, 2011; Knauer et al., 2017; Mao et al., 2015; Mu et al., 2011; Zeng et al., 2012; Zhang, Peña-Arancibia, et al., 2016). So far, no analysis has been conducted on the trends of GPP and ET components for sunlit and shaded leaf groups. Therefore, our analysis could reconcile some of the differences in the existing GPP and ET products. The objective of this study is to investigate the shifting roles of shaded and sunlit components of C and water fluxes under recent climate change. Specifically, we focus on the shaded part of these fluxes that are often considered as less important.

2 Materials and Methods

We use a two-leaf model, namely, the boreal ecosystem productivity simulator (BEPS) to calculate the coupled GPP and ET components at an

hourly time step (Chen et al., 1999, 2007, 2012; He et al., 2014; Ju et al., 2006; Liu et al., 1997). MERRA-2 (Modern-Era Retrospective Analysis for research and Applications, Version 2) data from Goddard Space Flight Center, NASA, are used to drive BEPS to simulate GPP and ET in 1981.7–2016.12 (Gelaro et al., 2017). The data have a spatial resolution of 0.625° (longitude) by 0.5° (latitude) and a temporal resolution of 1 hr. To drive BEPS, relative humidity, wind speed, and air temperature at 2 m above the surface, surface atmosphere pressure and incoming solar shortwave flux, and total precipitation at the surface level are spatially interpolated to the global 36 km EASE-Grid 2.0.

Two global leaf area index (LAI) products are used in this study. The first LAI product is a long-term consistent global LAI product (1981–2016, Version 3) that is retrieved from combined Advanced Very High Resolution Radiometer (AVHRR) and Moderate Resolution Imaging Spectroradiometer (MODIS) data sets (Liu et al., 2012). This product is generally referred to as GLOBMAP (Zhu et al., 2016). In Version 3, LAI from MODIS (Collection 6) has been corrected for sensor degradation and reprocessed using a new cloud screening algorithm (Y. Liu et al., 2012). The second LAI product is the Global Inventory Modeling and Mapping Studies (GIMMS) LAI3g that is produced using only AVHRR data (Zhu et al., 2013). The root-mean-square errors (RMSEs) for the two products are 0.81 and 0.68 LAI units, for GLOBMAP and GIMMS LAI3g, respectively. The LAI data are also reprojected to the 36-km resolution.

In BEPS, the canopy-level photosynthesis (A_{canopy}) is calculated as the sum of photosynthesis of sunlit and shaded leaf groups (Chen et al., 1999):

$$A_{canopy} = A_{sun} \cdot L_{sun} + A_{sh} \cdot L_{sh} \quad (1)$$

where the subscripts “sun” and “sh” denote the sunlit and shaded components of the photosynthesis (A) and LAI (L). The canopy-level ET is obtained as the sum of transpiration (T) and evaporation (E):

$$ET = T_{sun} \cdot L_{sun} + T_{sh} \cdot L_{sh} + E_l + E_g \quad (2)$$

where E_l and E_g are evaporation rates of intercepted water from canopy and ground surface, respectively.

The temperature response function of maximum carboxylation rate (V_{cmax}), the separation of sunlit and shaded LAI, the calculation of radiation and leaf temperature for each leaf group, and more detailed descriptions of the model and data are provided in the supporting information (Baldocchi, 1994; dePury & Farquhar, 1997; Friedl et al., 2002; He et al., 2012, 2016; Matsushita et al., 2004; Matsushita & Tamura, 2002; Medlyn et al., 1999; Monteith, 1965; Norman, 1982; Rienecker et al., 2011; Sellers et al., 1996; Sitch et al., 2008; Wang et al., 2004).

The BEPS-simulated GPP is validated against eddy covariance measurements from 124 flux tower sites (FLUXNET2015 Dataset in Tier 1;

http://fluxnet.fluxdata.org/) at the site level. Validation suggests that BEPS simulates annual GPP well with a coefficient of determinations (R^2) of 0.81, a RMSE of 347 g C $\cdot$ m^{-2} $\cdot$ $year^{-1}$, and a bias of 172 g C $\cdot$ m^{-2} $\cdot$ $year^{-1}$ (Figure S2).

3 Results and Discussion

In the following sections, we present trends of GPP and ET components using the Mann-Kendall test for the time frame of 1982–2016. We report the result based on GLOBMAP LAI product unless otherwise specified. In the following content, we report the averages of GPP and ET estimates along their one standard deviations (mean ± 1 SD) in 1982–2016. This one SD does not indicate an uncertainty estimate against observations; instead, it provides a relative change in the time series.

3.1 The Shift of Global and Regional GPP From the Shaded Leaf Group

With the GLOBMAP LAI (V3), the BEPS-simulated global GPP increases from 119.1 Pg C/year in 1982 to 133.2 Pg C/year in 2016 with an average of 124.4 ± 4.3 Pg C/year and a trend of 0.38 Pg C/year ($p < 0.01$; Figure 1); these estimates are close to recent report with a trend of 0.39 Pg C/year (2000–2016) and a global GPP of 129.4 Pg C/year in 2016 (Zhang, Xiao, Wu, et al., 2017). Comparing to the simulation using GLOBMAP LAI V2, the annual GPP estimates are consistently larger by 3 Pg C/year in 1982–2004, and since 2005, there is a significant growth in GPP driven by the LAI V3 with MODIS sensor degradation corrected (Figure S3). The consistent increase in simulated GPP is due to the removal of cloud-contaminated LAI retrievals that usually have low values. The growth in GPP driven by LAI V3 since 2005 is corresponding to the recent C budget imbalance (Figure S3) that is unexplained by other Earth system models (Le Quéré et al., 2017).

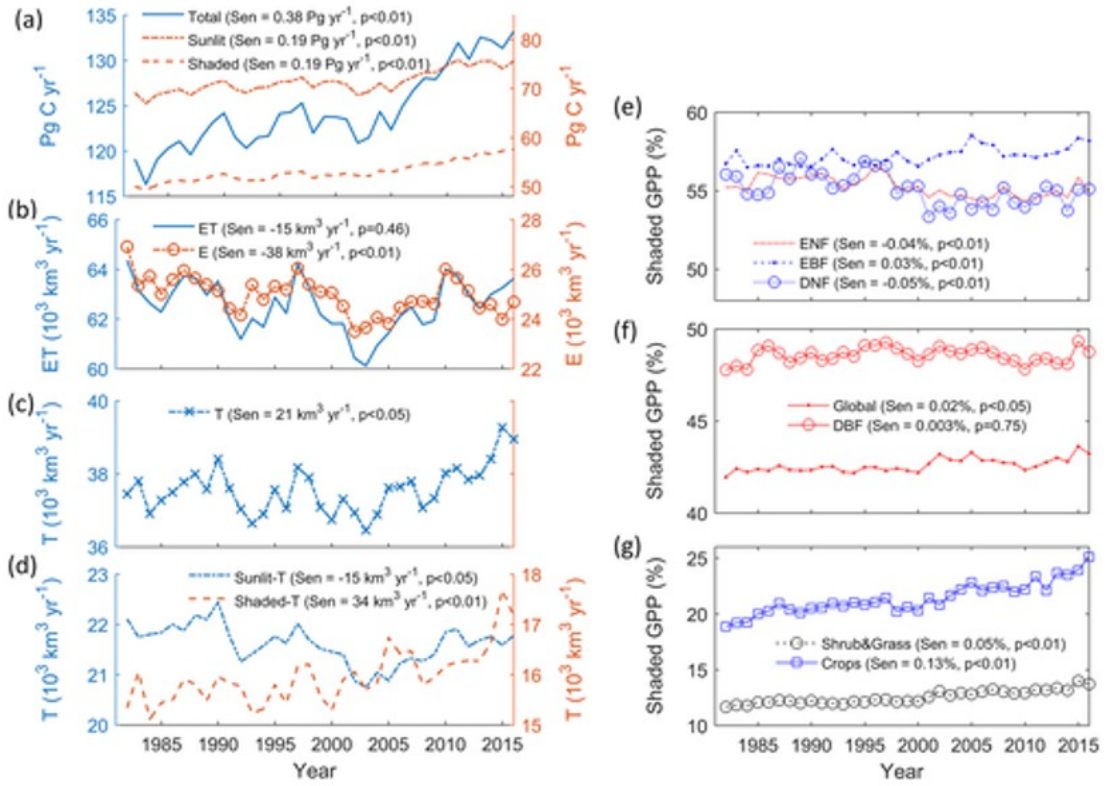

Figure 1

Time series of global gross primary production (GPP) and evapotranspiration (ET) components and the percentages of shaded GPP for different plant function types (ENF: evergreen needle leaf forest; EBF: evergreen broadleaf forest; DNF: deciduous needle leaf forest; DBF: deciduous broadleaf forest). (a) Global total GPP, GPP estimates from the sunlit and shaded groups, respectively. (b and c) Global total ET, evaporation (E), and transpiration (T). (d) Transpirations from the sunlit and shaded leaf groups. (e, f and g) Percentages of shaded GPP for different PFTs. “Sen” indicates Sen's slope in Mann-Kendall test. The simulation is conducted using GLOBMAP LAI product.

The sunlit GPP increases from 69.1 Pg C/year in 1982 to 75.6 Pg C/year in 2016 with an average of 71.4 ± 3.3 Pg C/year and a trend of 0.189 Pg C/year ($p < 0.01$), while the shaded GPP increases from 50.0 to 57.6 Pg C/year with an average of 53.0 ± 2.1 Pg C/year and a trend of 0.192 Pg C/year ($p < 0.01$). The fraction of shaded-to-total GPP increases from 42.0% to 43.2% with a trend of 0.02%/year ($p < 0.01$) during the same time frame. The shaded GPP fractions are slightly larger than the 39% found in a previous study (Chen et al., 2012). This change is due to an increase of understory LAI in BEPS according to Liu et al. (2017). Although the shaded GPP constitutes to less than a half of the total GPP, it contributes to more than a half of the total GPP increase (7.63 of 14.1 Pg C) since 1982, suggesting its increasing role in the global C cycle and budget.

There are considerable divergence among land cover types in terms of the fractions and trends of shaded GPP (Figure 1). Generally, shaded GPP contributes more to total GPP in forest ecosystems because of their large LAI (i.e., 55.2 ± 0.6%, 57.2 ± 0.5%, 55.1 ± 0.98%, and 48.6 ± 0.4% for

evergreen needleleaf forest [ENF], evergreen broadleaf forest [EBF], deciduous needleleaf forest [DNF], and deciduous broadleaf forest [DBF], respectively). Whereas, shaded GPP contributes less in the remaining terrestrial ecosystems (i.e., 12.5 ± 0.6%, and 21.4 ± 1.4% for shrub and grass and crops, respectively). In EBF, the fraction of shaded GPP has negligible change, while the shaded fractions in EBF (0.03%/year, $p < 0.01$), shrub and grass (0.05%/year, $p < 0.01$), and crops (0.13%/year, $p < 0.01$) follow increasing trends, and the shaded fractions in boreal forest have decreasing trends (−0.04%/year, $p < 0.01$, and −0.05%/year, $p < 0.01$ for ENF and DNF, respectively).

Two major drivers may lead to the shift in the shaded fraction of total GPP (Figure S1). The first is related to climate change. For example, an increase in air temperature near the surface causes an increase in leaf temperature, which may lead to increased or reduced shaded GPP fraction depending on the leaf temperature, that is, below or above the optimal photosynthesis temperature. In BEPS, a Boltzmann distribution is used to adjust the temperature responses of V_{cmax} and the maximum rate of electron transport (J_{max}) for photosynthesis (Baldocchi, 1994; Figure S1). Another driver is the change in LAI. When LAI is small (e.g., less than 1.5), the increase of LAI mostly contributes to an increase in sunlit LAI, while most of the increased LAI is shaded when the canopy is dense (Figure S1). Therefore, an increase of LAI may lead to different trends in the shaded GPP fractions. The causes of LAI changes may be CO_2 fertilization and/or nutrient availability. These two drivers may be coupled in an ecosystem. Therefore, we only report the integral changes in the shaded GPP fraction in this letter and leave the quantitative attribution of drivers for subsequent studies.

In tropical rainforests located at Amazon and central Africa, we found declining sunlit GPP trends, which were compensated by increasing shaded GPP trends (Figure S4). The decline of sunlit GPP is unlikely due to reduction in LAI since the LAI in these regions is as high as 8. Therefore, climate change (e.g., warming) may be the driver for this decline (Peñuelas et al., 2017). The increases of the shaded GPP trend and its fraction (Figure 2) suggest that the shaded leaf group offsets the decline of sunlit GPP and plays an increasing role in mitigating the adverse warming effect in the tropical area (Brienen et al., 2015). The increase in the shaded GPP fraction also provides a niche for a potential evolution in canopy structure in the tropical forests that have already been observed (Cernusak et al., 2013; Cusack et al., 2016; Feeley et al., 2011, 2013; Morueta-Holme et al., 2015; Slot & Winter, 2016). In the near future, if climate warming continues, the rainforests will be exposed to air temperatures that are even higher than the optimal temperature for photosynthesis (Cavaleri et al., 2015; Peñuelas et al., 2017). Our study suggests that a more clumped canopy structure (with more shaded leaves) is in favor of tropical ecosystem productivity and provides resilience to over-warming in the future. The trend in the fraction of shaded GPP in South Asian tropical forests is insignificant, suggesting that it

may also be affected by other drivers (e.g., nitrogen deposition due to agricultural fertilizer use).

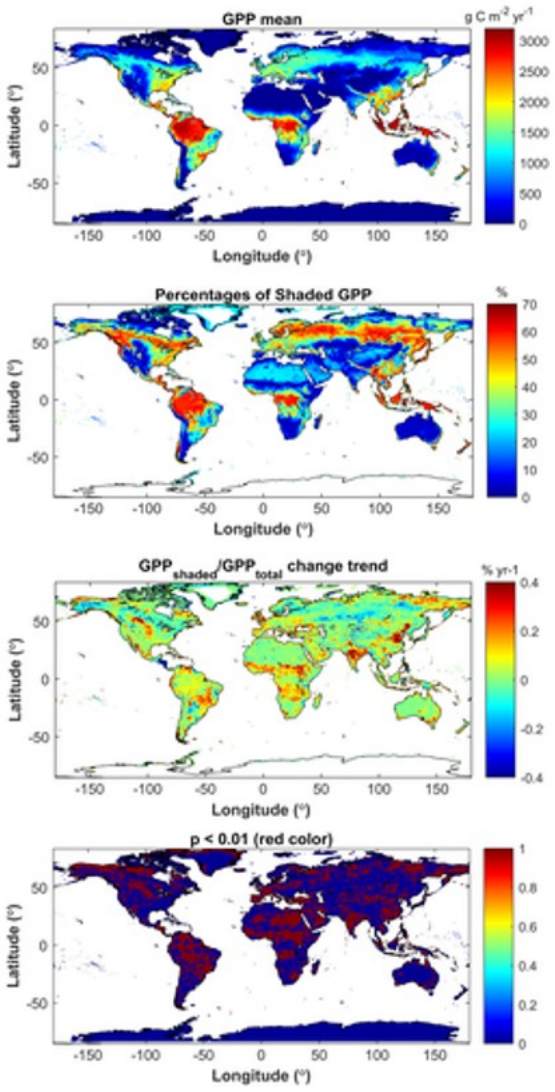

Figure 2

(first panel) Global distributions of annual GPP averaged in 1982–2016, (second panel) the percentages of shaded GPP, and (third and fourth panels) the change trend in the fraction of shaded GPP and its significance, where the positive trend indicates that the fraction of shaded GPP is increasing (third panel). The simulation is conducted using GLOBMAP LAI product.

In DNF and ENF boreal forests, we found that the trend of sunlit GPP is positive while the trend of shaded GPP is close to neutral (Figure S4), suggesting that climate warming at high latitudes has more effect on sunlit leaves than on shaded leaves. Boreal conifers have adapted to the cold climate with narrow conical tree crowns to shed snow in winter, and their evergreen needles have an advantage in maximizing the growing season length in the cold climate. However, the clumped canopy structure reduces the fraction of leaves exposed to direct sunlight (i.e., sunlit leaves). Under

global warming, this cold adaptation of boreal conifer canopies could lose out to deciduous forests that have less clumped canopies to receive more direct sunlight. Our study helps explain the observed northward shift of boreal forests (Boulanger et al., 2017; Girardin et al., 2016; Savage & Vellend, 2015).

The variations of annual global GPP and ET are strongly modulated by El Niño-Southern Oscillation that causes climate extremes (Cavaleri et al., 2017). By separating shaded from sunlit GPP, we found that both absolute and relative variations of shaded GPP are less than that of sunlit GPP (0.83 Pg C, or 1.5% for shaded GPP, and 1.34 Pg C, or 1.9% for sunlit GPP, in terms of one standard deviation, after their linear trends are removed from their time series), suggesting that shaded GPP is less affected by El Niño-Southern Oscillation.

3.2 The Accompanied Change in Shaded ET

There are large discrepancies of the global ET estimates, in terms of their trends and variabilities (Anabalon & Sharma, 2017; Dong & Dai, 2017; Shi et al., 2013; Ukkola & Prentice, 2013; Zeng et al., 2014); the reported trends can also be affected by the starting and ending years (Zeng et al., 2012). Separating the ET components help to identify their different drives under climate change (Zhang, Xiao, Zhou, et al., 2017) and reconcile the differences among ET products; for example, rising CO_2 improves WUE and yields decreasing trend in canopy transpiration (Mao et al., 2015; Zhang, Peña-Arancibia, et al., 2016), while this decreasing trend may be compensated by the Earth's greening (Zeng et al., 2016). The trivial and divergent trends of global ET products may be attributed to uncertainties in fractions of ET components.

In this study, the global ET simulated by BEPS (Figures 1 and S5) decreases from 64.4×10^3 km^3/year in 1982 to 63.6×10^3 km^3/year in 2016 with an average of $62.5 \pm 1.0 \times 10^3$ km^3/year and an insignificant trend of -0.015×10^3 km^3/year ($p = 0.46$). The ET estimates in the first few years may be affected by model spin-up. Our simulation is close to the estimate (63.2×10^3 km^3/year in 1982–2012) by observation-driven Penman-Monteith-Leuning (PML) model (Zhang, Peña-Arancibia, et al., 2016). Using PML model as reference, our simulation has a R^2 of 0.89, uRMSE of 107 mm/year, and bias of −29.9 mm/year. While this global trend is insignificant, we found that the trends of ET components are much clearer: the global evaporation decreases from 26.9×10^3 km^3/year in 1982 to 24.7×10^3 km^3/year in 2016 with an average of $25.0 \pm 0.7 \times 10^3$ km^3/year and a trend of -0.038×10^3 km^3/year ($p < 0.01$); the global transpiration increases from 37.4×10^3 km^3/year in 1982 to 38.9×10^3 km^3/year with an average of $37.6 \pm 0.6 \times 10^3$ km^3/year and a trend of 0.021×10^3 km^3/year ($p < 0.05$). Transpiration accounts for 60.2% of global ET from our simulation, similar to the value (61%) estimated from a compilation of 81 studies (Schlesinger & Jasechko, 2014), the estimate (64%) by Good et al. (2015), and the estimate (57.2%) by Wei et al.

(2017). Should the ratio of transpiration from our simulation have more weight, the estimated global ET trend can be reversed. Our study echoes the result by Zhang, Peña-Arancibia, et al. (2016), which shows opposing trends in E and T. Therefore, we suggest that both the ratio and the trends of ET components are reported in future studies.

Separating global transpiration for the sunlit and shaded leaf groups (T_s and T_{sh}) reveals even more information: the T_s and T_{sh} also show opposite trends (Figure 1). T_s decreases from 22.1 × 10^3 km^3/year in 1982 to 21.8 × 10^3 km^3/year in 2016 with an average of 21.6 ± 0.4 × 10^3 km^3/year and a trend of −0.015 × 10^3 km^3/year ($p < 0.05$), while the T_{sh}increases from 15.3 × 10^3 km^3/year in 1982 to 17.2 × 10^3 km^3/year in 2016 with an average of 16.0 ± 0.5 × 10^3 km^3/year and a trend of 0.034 × 10^3 km^3/year ($p < 0.01$). Globally, forests with large LAI values contribute most of the ET. Since sunlit LAI in forests is less sensitive to the Earth's greening, the decreasing trend of T_s may be more attributed to improved WUE due to rising CO_2. Accompanying the growing of shaded GPP, shaded leaves contribute most of the increasing trend in global transpiration; the greening may contribute more than WUE for the increasing T_{sh} trend.

Notably, the significance of T_s trend ($p < 0.05$) is less than that of T_{sh} ($p < 0.01$). Separating between T_s and T_{sh} enables us to find an important turning point (year 2003) in the time series of T_s as suggested by M. Jung et al. (2010) due to limited soil moisture supply: $T_s$decreases significantly from 1982 to 2003 (−0.037 × 10^3 km^3/year, $p < 0.01$) and also increases significantly since then (0.065 × 10^3 km^3/year, $p < 0.01$), while T_{sh} has a consistent increasing trend in 1982–2016. Therefore, the turning point, connecting two significant but opposite trends, explains the low significance of T_s trend. The turning point in T_s is also useful to reconcile the global ET trends from different ET products: the sign of ET trend may change depending on the starting and ending years of a specific period in different studies. There is no turning point in T_{sh} due to the same soil moisture supply; possible reasons include the following: (1) transpiration from shaded leaves is less affected by water stress (Barradas et al., 2005; Nicolas et al., 2008; Pepin et al., 2002) and (2) strong greening trend in LAI has more effect on shaded leaves and overrides the turning point in T_{sh}. Clearly, T_{sh}dominates the increasing trend of the total T. In contrast to GPP, we found that T_{sh}(0.39 × 10^3 km^3, or 2.5%) has larger interannual variations than T_s (0.35 × 10^3 km^3, or 1.6%) after the linear trend is removed.

The fraction of global transpiration (T divided by ET) increases from 41.0% in 1982 to 44.1% in 2016 with an average of 42.5 ± 1.0% and an increasing trend of 0.07%/year ($p < 0.01$). The fraction of T_{sh} (T_{sh} divided by T) is similar to the fraction of shaded GPP (Figure 1). The fractions of T_{sh} are 51.4 ± 0.7%, 56.1 ± 1.3%, 52.1 ± 1.0%, 48.0 ± 0.7%, 14.8 ± 0.7%, and 23.6 ± 1.4% for ENF, EBF, DNF, DBF, shrub and grass, and crops, respectively. The change in the trend of the fraction of T_{sh} is insignificant for ENF ($p = 0.16$) and DNF ($p = 0.86$) in boreal forests (Figure S6). All other land cover types show an

increasing trend of T_{sh} (0.09%/year and $p < 0.01$, 0.04%/year and $p < 0.01$, 0.06%/year and $p < 0.01$, and 0.13%/year and $p < 0.01$ for EBF, DBF, shrub and grass, and crops, respectively). Similar to the increasing trend of the fraction of shaded GPP, our study suggests that T_{sh} also has an increasing role in the global water cycle.

3.3 Uncertainties

Climate reanalysis data are the outputs of Earth system models that assimilate various archived observations. Global reanalysis data are the best available data sets for this study. Recent validation suggests that MERRA2 data sets have relatively small errors comparing to a few other reanalysis data sets (Draper et al., 2018; Eyre & Zeng, 2017; Reichle, Liu, et al., 2017; Reichle, Draper, et al., 2017; Simmons et al., 2017). However, further studies are still needed to reduce the uncertainties of trend analysis from forcing data.

The GPP and ET trends may also be affected by different LAI products. In this study, we compared the result based on GLOBMAP LAI to simulation based on GIMMS LAI3g. We found consistent results except at conifer forests (Figures S7–S12). Compared to other land covers, conifer forests have one extra clumping effect within shoots (Chen et al., 1997). The clumping effect within shoots is explained in the GLOBMAP using a clumping index map (He et al., 2012), while this effect is uncorrected in the LAI3g product yet. Therefore, we found that the ratio of shaded GPP from conifers based on LAI3g is less than that simulated using GLOBMAP. Correspondingly, we found that ratios of shaded GPP in ENF and DNF are still in decreasing trends, but the trends are insignificant from the LAI3g product.

4 Conclusions

The changing ambient temperature and CO_2 concentration, together with radiation and water and nutrient availability, can greatly alter C and water fluxes in terrestrial ecosystems. Exposed to diffuse radiation only, the shaded part of a canopy has lower temperature than the sunlit part; therefore, shaded and sunlit leaves will have different responses to climate change. We used a two-leaf modeling approach to investigate the changing role of shaded leaves under climate change in terms of photosynthesis and transpiration during 1982–2016. We found that globally shaded leaves contribute 42.6 ± 0.4% of the total GPP (124.4 ± 4.3 Pg C/year). However, shaded GPP and sunlit GPP share a similar increasing trend (0.19 Pg C/year, $p < 0.01$); therefore, shaded leaves contribute to half the total GPP increase (7.6 Pg C) during the 35-year period. Due to different dependence of leaf temperature on V_{cmax}, the proportion of shaded GPP increases in tropical forests (0.03%/year, $p < 0.01$) and decreases in boreal forests (−0.04%/year for ENFs with $p < 0.01$ and −0.05%/year for DNFs with $p < 0.01$), suggesting a potential shift in canopy structure for ecosystems to achieve maximum GPP. By differentiating transpiration between shaded (T_{sh}) and sunlit leaves (T_s), we identified that T_{sh} has an increasing trend of 0.034×10^3 km^3/year (p

< 0.01), while T_s has a sharp turning point in the trend due to change of moisture supply, with a decreasing trend of -0.037×10^3 km^3/year ($p < 0.01$) in 1982–2003, followed by an increasing trend of 0.065×10^3 km^3/year ($p < 0.01$) in 2004–2016. According to our simulation, global GPP from shaded leaves is less susceptible to climate warming, compared to their sunlit counterparts. Our study clearly suggests that the shaded leaf group has an increasing role during the last three and a half decades.

The uncertainties from the MERRA2 forcing data, LAI product, and land cover and land change products, model parameters, and other missing drives that may cause effects in capturing the GPP and ET trends are data source specific, difficult to quantify, and cannot be ruled out.

Acknowledgments

This study was supported by the Canadian Space Agency grant (14SUSMAPTO). This work used eddy covariance data acquired and shared by the FLUXNET community, including AmeriFlux, AfriFlux, AsiaFlux, CarboAfrica, CarboEuropeIP, CarboItaly, CarboMont, ChinaFlux, Fluxnet-Canada, GreenGrass, ICOS, KoFlux, LBA, NECC, OzFlux-TERN, TCOS-Siberia, and USCCC. The ERA-Interim reanalysis data are provided by ECMWF and processed by LSCE. The FLUXNET data processing and harmonization were carried out by the European Fluxes Database Cluster, AmeriFlux Management Project, and Fluxdata project of FLUXNET, with the support of CDIAC and ICOS Ecosystem Thematic Center, and the OzFlux, ChinaFlux, and AsiaFlux offices. The data used are listed in the supporting information.

References

Alarcon, J. J., Ortuno, M. F., Nicolas, E., Navarro, A., & Torrecillas, A. (2006). Improving water-use efficiency of young lemon trees by shading with aluminised-plastic nets. *Agricultural Water Management*, 82(3), 387– 398. https://doi.org/10.1016/j.agwat.2005.08.003

Amissah, L., Mohren, G. M. J., Kyereh, B., & Poorter, L. (2015). The effects of drought and shade on the performance, morphology and physiology of Ghanaian tree species. *PLoS One*, 10(4), e0121004. https://doi.org/10.1371/journal.pone.0121004

Anabalon, A., & Sharma, A. (2017). On the divergence of potential and actual evapotranspiration trends: An assessment across alternate global datasets. *Earths Future*, 5(9), 905– 917. https://doi.org/10.1002/2016EF000499

Anav, A., Friedlingstein, P., Beer, C., Ciais, P., Harper, A., Jones, C., et al. (2015). Spatiotemporal patterns of terrestrial gross primary production: A review. *Reviews of Geophysics*, 53(3), 785– 818. https://doi.org/10.1002/2015RG000483

Ashton, P. M. S., & Berlyn, G. P. (1992). Leaf adaptations of some Shorea species to Sun and shade. *New Phytologist*, 121(4), 587– 596. https://doi.org/10.1111/j.1469-8137.1992.tb01130.x

Baldocchi, D. (1994). An analytical solution for coupled leaf photosynthesis and stomatal conductance models. *Tree Physiology*, 14(7-8-9), 1069– 1079. https://doi.org/10.1093/treephys/14.7-8-9.1069

Ball, J., Woodrow, L. E., & Beny, J. A. (1987). A model predicting stomatal conductance and its contribution to the control of photosynthesis under different environmental conditions. In J. Biggins (Ed.), *Progress in Photosynthesis research* (Vol. 4, pp. 221– 224). Dordrecht: Nijhoff.

Barradas, V. L., Nicolas, E., Torrecillas, A., & Alarcon, J. J. (2005). Transpiration and canopy conductance in young apricot (*Prunus armenica* L.) trees subjected to different PAR levels and water stress. *Agricultural Water Management*, 77(1–3), 323– 333. https://doi.org/10.1016/j.agwat.2004.09.035

Beer, C., Reichstein, M., Tomelleri, E., Ciais, P., Jung, M., Carvalhais, N., et al. (2010). Terrestrial gross carbon dioxide uptake: Global distribution and covariation with climate. *Science*, 329(5993), 834– 838. https://doi.org/10.1126/science.1184984

Bonan, G. B., Williams, M., Fisher, R. A., & Oleson, K. W. (2014). Modeling stomatal conductance in the earth system: Linking leaf water-use efficiency and water transport along the soil-plant-atmosphere continuum. *Geoscientific Model Development*, 7(5), 2193– 2222. https://doi.org/10.5194/gmd-7-2193-2014

Boulanger, Y., Taylor, A. R., Price, D. T., Cyr, D., McGarrigle, E., Rammer, W., et al. (2017). Climate change impacts on forest landscapes along the Canadian southern boreal forest transition zone. *Landscape Ecology*, 32(7), 1415– 1431. https://doi.org/10.1007/s10980-016-0421-7

Brienen, R. J. W., Phillips, O. L., Feldpausch, T. R., Gloor, E., Baker, T. R., Lloyd, J., et al. (2015). Long-term decline of the Amazon carbon sink. *Nature*, 519(7543), 344.

Cavaleri, M. A., Coble, A. P., Ryan, M. G., Bauerle, W. L., Loescher, H. W., & Oberbauer, S. F. (2017). Tropical rainforest carbon sink declines during El Nino as a result of reduced photosynthesis and increased respiration rates. *New Phytologist*, 216(1), 136– 149. https://doi.org/10.1111/nph.14724

Cavaleri, M. A., Reed, S. C., Smith, W. K., & Wood, T. E. (2015). Urgent need for warming experiments in tropical forests. *Global Change Biology*, 21(6), 2111– 2121. https://doi.org/10.1111/gcb.12860

Cernusak, L. A., Winter, K., Dalling, J. W., Holtum, J. A. M., Jaramillo, C., Korner, C., et al. (2013). Tropical forest responses to increasing atmospheric CO_2: Current knowledge and opportunities for future research. *Functional Plant Biology*, 40(6), 531– 551. https://doi.org/10.1071/FP12309

Chen, B., Chen, J. M., & Ju, W. (2007). Remote sensing-based ecosystem–atmosphere simulation scheme (EASS)—Model formulation and test with

multiple-year data. *Ecological Modelling*, 209(2–4), 277– 300. https://doi.org/10.1016/j.ecolmodel.2007.06.032

Chen, B., Liu, J., Chen, J. M., Croft, H., Gonsamo, A., He, L., & Luo, X. (2016). Assessment of foliage clumping effects on evapotranspiration estimates in forested ecosystems. *Agricultural and Forest Meteorology*, 216, 82– 92. https://doi.org/10.1016/j.agrformet.2015.09.017

Chen, J. M., Liu, J., Cihlar, J., & Goulden, M. L. (1999). Daily canopy photosynthesis model through temporal and spatial scaling for remote sensing applications. *Ecological Modelling*, 124(2–3), 99– 119. https://doi.org/10.1016/S0304-3800(99)00156-8

Chen, J. M., Mo, G., Pisek, J., Liu, J., Deng, F., Ishizawa, M., & Chan, D. (2012). Effects of foliage clumping on the estimation of global terrestrial gross primary productivity. *Global Biogeochemical Cycles*, 26, GB1019. https://doi.org/10.1029/2010GB003996

Chen, J. M., Rich, P. M., Gower, S. T., Norman, J. M., & Plummer, S. (1997). Leaf area index of boreal forests: Theory, techniques, and measurements. *Journal of Geophysical Research*, 102(D24), 29,429– 29,443. https://doi.org/10.1029/97JD01107

Chen, M., Rafique, R., Asrar, G. R., Bond-Lamberty, B., Ciais, P., Zhao, F., et al. (2017). Regional contribution to variability and trends of global gross primary productivity. *Environmental Research Letters*, 12(10). https://doi.org/10.1088/1748-9326/aa8978

Cusack, D. F., Karpman, J., Ashdown, D., Cao, Q., Ciochina, M., Halterman, S., et al. (2016). Global change effects on humid tropical forests: Evidence for biogeochemical and biodiversity shifts at an ecosystem scale. *Reviews of Geophysics*, 54, 523– 610. https://doi.org/10.1002/2015RG000510

Dai, Y. J., Dickinson, R. E., & Wang, Y. P. (2004). A two-big-leaf model for canopy temperature, photosynthesis, and stomatal conductance. *Journal of Climate*, 17(12), 2281– 2299. https://doi.org/11520-0442(1996)009/1520-0442(2004)017%3C2281:Atmfct%3E2.0.Co;2

de Casas, R. R., Vargas, P., Perez-Corona, E., Manrique, E., Garcia-Verdugo, C., & Balaguer, L. (2011). Sun and shade leaves of Olea europaea respond differently to plant size, light availability and genetic variation. *Functional Ecology*, 25(4), 802– 812. https://doi.org/10.1111/j.1365-2435.2011.01851.x

dePury, D. G. G., & Farquhar, G. D. (1997). Simple scaling of photosynthesis from leaves to canopies without the errors of big-leaf models. *Plant, Cell and Environment*, 20(5), 537– 557. https://doi.org/10.1111/j.1365-3040.1997.00094.x

Dong, B., & Dai, A. (2017). The uncertainties and causes of the recent changes in global evapotranspiration from 1982 to 2010. *Climate Dynamics*, 49(1-2), 279– 296. https://doi.org/10.1007/s00382-016-3342-x

Drake, B. L., Hanson, D. T., Lowrey, T. K., & Sharp, Z. D. (2017). The carbon fertilization effect over a century of anthropogenic CO_2 emissions: Higher intracellular CO_2 and more drought resistance among invasive and native grass species contrasts with increased water use efficiency for woody plants in the US southwest. *Global Change Biology*, 23(2), 782– 792. https://doi.org/10.1111/gcb.13449

Draper, C. S., Reichle, R. H., & Koster, R. D. (2018). Assessment of MERRA-2 land surface energy flux estimates. *Journal of Climate*, 31(2), 671– 691. https://doi.org/1520-0442(1996)009%3C0676/JCLI-D-17-0121.1

Drewry, D. T., Kumar, P., & Long, S. P. (2014). Simultaneous improvement in productivity, water use, and albedo through crop structural modification. *Global Change Biology*, 20(6), 1955– 1967. https://doi.org/10.1111/gcb.12567

Eyre, J. E. J. R., & Zeng, X. B. (2017). Evaluation of Greenland near surface air temperature datasets. *The Cryosphere*, 11(4), 1591– 1605. https://doi.org/10.5194/tc-11-1591-2017

Farquhar, G. D., Caemmerer, S. V., & Berry, J. A. (1980). A biochemical-model of photosynthetic CO_2 assimilation in leaves of C-3 species. *Planta*, 149(1), 78– 90. https://doi.org/10.1007/Bf00386231

Feeley, K. J., Davies, S. J., Perez, R., Hubbell, S. P., & Foster, R. B. (2011). Directional changes in the species composition of a tropical forest. *Ecology*, 92(4), 871– 882. https://doi.org/10.1890/10-0724.1

Feeley, K. J., Hurtado, J., Saatchi, S., Silman, M. R., & Clark, D. B. (2013). Compositional shifts in Costa Rican forests due to climate-driven species migrations. *Global Change Biology*, 19(11), 3472– 3480. https://doi.org/10.1111/gcb.12300

Friedl, M. A., McIver, D. K., Hodges, J. C. F., Zhang, X. Y., Muchoney, D., Strahler, A. H., et al. (2002). Global land cover mapping from MODIS: Algorithms and early results. *Remote Sensing of Environment*, 83(1–2), 287– 302. https://doi.org/10.1016/S0034-4257(02)00078-0

Gelaro, R., McCarty, W., Suarez, M. J., Todling, R., Molod, A., Takacs, L., et al. (2017). The Modern-Era Retrospective Analysis for Research and Applications, Version 2 (MERRA-2). *Journal of Climate*, 30(14), 5419– 5454. https://doi.org/10.1175/JCLI-D-16-0758.1

Girardin, M. P., Hogg, E. H., Bernier, P. Y., Kurz, W. A., Guo, X. J., & Cyr, G. (2016). Negative impacts of high temperatures on growth of black spruce forests intensify with the anticipated climate warming. *Global Change Biology*, 22(2), 627– 643. https://doi.org/10.1111/gcb.13072

Goddard Institute for Space Studies Surface Temperature Analysis (2017). GISS Surface Temperature Analysis. Retrieved from https://data.giss.nasa.gov/gistemp/

Good, S. P., Noone, D., & Bowen, G. (2015). Hydrologic connectivity constrains partitioning of global terrestrial water fluxes. *Science*, 349(6244), 175– 177. https://doi.org/10.1126/science.aaa5931

Hansen, J., Ruedy, R., Sato, M., & Lo, K. (2010). Global surface temperature change. *Reviews of Geophysics*, 48, RG4004. https://doi.org/10.1029/2010RG000345

He, L., Chen, J. M., Liu, J., Bélair, S., & Luo, X. (2017). Assessment of SMAP soil moisture for global simulation of gross primary production. *Journal of Geophysical Research: Biogeosciences*, 122, 1549– 1563. https://doi.org/10.1002/2016JG003603

He, L., Chen, J. M., Liu, J., Mo, G., Bélair, S., Zheng, T., et al. (2014). Optimization of water uptake and photosynthetic parameters in an ecosystem model using tower flux data. *Ecological Modelling*, 294, 94– 104. https://doi.org/10.1016/j.ecolmodel.2014.09.019

He, L., Chen, J. M., Pisek, J., Schaaf, C. B., & Strahler, A. H. (2012). Global clumping index map derived from the MODIS BRDF product. *Remote Sensing of Environment*, 119, 118– 130. https://doi.org/10.1016/j.rse.2011.12.008

He, L. M., Chen, J. M., Croft, H., Gonsamo, A., Luo, X. Z., Liu, J. N., et al. (2017). Nitrogen availability dampens the positive impacts of CO_2 fertilization on terrestrial ecosystem carbon and water cycles. *Geophysical Research Letters*, 44, 11,590– 11,600. https://doi.org/10.1002/2017gl075981

He, L. M., Liu, J., Chen, J. M., Croft, H., Wang, R., Sprintsin, M., et al. (2016). Inter- and intra-annual variations of clumping index derived from the MODIS BRDF product. *International Journal of Applied Earth Observation and Geoinformation*, 44, 53– 60. https://doi.org/10.1016/j.jag.2015.07.007

Jiang, C., & Ryu, Y. (2016). Multi-scale evaluation of global gross primary productivity and evapotranspiration products derived from Breathing Earth System Simulator (BESS). *Remote Sensing of Environment*, 186, 528– 547. https://doi.org/10.1016/j.rse.2016.08.030

Ju, W., Chen, J. M., Black, T. A., Barr, A. G., Liu, J., & Chen, B. (2006). Modelling multi-year coupled carbon and water fluxes in a boreal aspen forest. *Agricultural and Forest Meteorology*, 140(1–4), 136– 151. https://doi.org/10.1016/j.agrformet.2006.08.008

Jung, M., Reichstein, M., Ciais, P., Seneviratne, S. I., Sheffield, J., Goulden, M. L., et al. (2010). Recent decline in the global land evapotranspiration trend due to limited moisture supply. *Nature*, 467(7318), 951– 954. https://doi.org/10.1038/nature09396

Jung, M., Reichstein, M., Margolis, H. A., Cescatti, A., Richardson, A. D., Arain, M. A., et al. (2011). Global patterns of land-atmosphere fluxes of carbon dioxide, latent heat, and sensible heat derived from eddy covariance, satellite, and meteorological observations. *Journal of Geophysical Research*, 116, G00J07. https://doi.org/10.1029/2010JG001566

Keenan, T. F., & Niinemets, Ü. (2016). Global leaf trait estimates biased due to plasticity in the shade. *Nature Plants*, 3, 16201. https://doi.org/10.1038/nplants.2016.201

Knauer, J., Zaehle, S., Reichstein, M., Medlyn, B. E., Forkel, M., Hagemann, S., & Werner, C. (2017). The response of ecosystem water-use efficiency to rising atmospheric CO2 concentrations: Sensitivity and large-scale biogeochemical implications. *New Phytologist*, 213(4), 1654– 1666. https://doi.org/10.1111/nph.14288

Landry, J. S., Partanen, A. I., & Matthews, H. D. (2017). Carbon cycle and climate effects of forcing from fire-emitted aerosols. *Environmental Research Letters*, 12(2), 025002. https://doi.org/10.1088/1748-9326/aa51de

Le Quéré, C., Andrew, R. M., Friedlingstein, P., Sitch, S., Pongratz, J., Manning, A. C., et al. (2017). Global carbon budget 2017. *Earth System Science Data Discussions*, 2017, 1– 79. https://doi.org/10.5194/essd-2017-123

Liu, J., Chen, J. M., Cihlar, J., & Park, W. M. (1997). A process-based boreal ecosystem productivity simulator using remote sensing inputs. *Remote Sensing of Environment*, 62(2), 158– 175. https://doi.org/10.1016/S0034-4257(97)00089-8

Liu, Y., Liu, R., Pisek, J., & Chen, J. M. (2017). Separating overstory and understory leaf area indices for global needleleaf and deciduous broadleaf forests by fusion of MODIS and MISR data. *Biogeosciences*, 14(5), 1093– 1110. https://doi.org/10.5194/bg-14-1093-2017

Liu, Y., Liu, R. G., & Chen, J. M. (2012). Retrospective retrieval of long-term consistent global leaf area index (1981–2011) from combined AVHRR and MODIS data. *Journal of Geophysical Research*, 117, G04003. https://doi.org/10.1029/2012JG002084

Lu, X., Chen, M., Liu, Y., Miralles, D. G., & Wang, F. (2017). Enhanced water use efficiency in global terrestrial ecosystems under increasing aerosol loadings. *Agricultural and Forest Meteorology*, 237-238(supplement C), 39– 49. https://doi.org/10.1016/j.agrformet.2017.02.002

Luo, X. Z., Chen, J. M., Liu, J. E., Black, T. A., Croft, H., Staebler, R., et al. (2018). Comparison of big-leaf, two-big-leaf, and two-leaf upscaling schemes for evapotranspiration estimation using coupled carbon-water modeling. *Journal of Geophysical Research: Biogeosciences*, 123, 207– 225. https://doi.org/10.1002/2017jg003978

Maestre, F. T., Eldridge, D. J., Soliveres, S., Kefi, S., Delgado-Baquerizo, M., Bowker, M. A., et al. (2016). Structure and functioning of dryland ecosystems in a changing world. *Annual Review of Ecology, Evolution, and Systematics*, 47(1), 215– 237. https://doi.org/10.1146/annurev-ecolsys-121415-032311

Mao, J. F., Fu, W. T., Shi, X. Y., Ricciuto, D. M., Fisher, J. B., Dickinson, R. E., et al. (2015). Disentangling climatic and anthropogenic controls on global

terrestrial evapotranspiration trends. *Environmental Research Letters*, 10(9), 094008. https://doi.org/10.1088/1748-9326/10/9/094008

Martins, S. C. V., Galmes, J., Cavatte, P. C., Pereira, L. F., Ventrella, M. C., & DaMatta, F. M. (2014). Understanding the low photosynthetic rates of Sun and shade coffee leaves: Bridging the gap on the relative roles of hydraulic, diffusive and biochemical constraints to photosynthesis. *PLoS One*, 9(4), e95571. https://doi.org/10.1371/journal.pone.0095571

Matsushita, B., & Tamura, M. (2002). Integrating remotely sensed data with an ecosystem model to estimate net primary productivity in East Asia. *Remote Sensing of Environment*, 81(1), 58– 66. https://doi.org/10.1016/S0034-4257(01)00331-5

Matsushita, B., Xu, M., Chen, J., Kameyama, S., & Tamura, M. (2004). Estimation of regional net primary productivity (NPP) using a process-based ecosystem model: How important is the accuracy of climate data? *Ecological Modelling*, 178(3–4), 371– 388. https://doi.org/10.1016/j.ecolmodel.2004.03.012

Mazdiyasni, O., & AghaKouchak, A. (2015). Substantial increase in concurrent droughts and heatwaves in the United States. *Proceedings of the National Academy of Sciences of the United States of America*, 112(37), 11,484–11,489. https://doi.org/10.1073/pnas.1422945112

McCluney, K. E., Belnap, J., Collins, S. L., Gonzalez, A. L., Hagen, E. M., Holland, J. N., et al. (2012). Shifting species interactions in terrestrial dryland ecosystems under altered water availability and climate change. *Biological Reviews*, 87(3), 563– 582. https://doi.org/10.1111/j.1469-185X.2011.00209.x

Medlyn, B. E., Badeck, F. W., De Pury, D. G. G., Barton, C. V. M., Broadmeadow, M., Ceulemans, R., et al. (1999). Effects of elevated [CO2] on photosynthesis in European forest species: A meta-analysis of model parameters. *Plant, Cell and Environment*, 22(12), 1475– 1495. https://doi.org/10.1046/j.1365-3040.1999.00523.x

Millar, R. J., Fuglestvedt, J. S., Friedlingstein, P., Rogelj, J., Grubb, M. J., Matthews, H. D., et al. (2017). Emission budgets and pathways consistent with limiting warming to 1.5 degrees C. *Nature Geoscience*, 10(10), 741.

Montanaro, G., Dichio, B., & Xiloyannis, C. (2009). Shade mitigates photoinhibition and enhances water use efficiency in kiwifruit under drought. *Photosynthetica*, 47(3), 363– 371. https://doi.org/10.1007/s11099-009-0057-9

Monteith, J. L. (1965). Evaporation and environment. *Symposia of the Society for Experimental Biology*, 19, 205– 224.

Morueta-Holme, N., Engemann, K., Sandoval-Acuna, P., Jonas, J. D., Segnitz, R. M., & Svenning, J. C. (2015). Strong upslope shifts in Chimborazo's vegetation over two centuries since Humboldt. *Proceedings of the National*

Academy of Sciences of the United States of America, 112(41), 12,741–12,745. https://doi.org/10.1073/pnas.1509938112

Mu, Q., Zhao, M., & Running, S. W. (2011). Improvements to a MODIS global terrestrial evapotranspiration algorithm. *Remote Sensing of Environment*, 115(8), 1781– 1800. https://doi.org/10.1016/j.rse.2011.02.019

Nicolas, E., Barradas, V. L., Ortuno, M. F., Navarro, A., Torrecillas, A., & Alarcon, J. J. (2008). Environmental and stomatal control of transpiration, canopy conductance and decoupling coefficient in young lemon trees under shading net. *Environmental and Experimental Botany*, 63(1–3), 200– 206. https://doi.org/10.1016/j.envexpbot.2007.11.007

Norman, J. M. (1982). Simulation of microclimates. In H. Jerry (Ed.), *Biometeorology in Integrated Pest Management* (pp. 65– 99). New York: Academic Press.

Pecl, G. T., Araujo, M. B., Bell, J. D., Blanchard, J., Bonebrake, T. C., Chen, I. C., et al. (2017). Biodiversity redistribution under climate change: Impacts on ecosystems and human well-being. *Science*, 355(6332), 1389.

Peñuelas, J., Ciais, P., Canadell, J. G., Janssens, I. A., Fernández-Martínez, M., Carnicer, J., et al. (2017). Shifting from a fertilization-dominated to a warming-dominated period. *Nature Ecology & Evolution*, 1(10), 1438– 1445. https://doi.org/10.1038/s41559-017-0274-8

Pepin, S., Livingston, N. J., & Whitehead, D. (2002). Responses of transpiration and photosynthesis to reversible changes in photosynthetic foliage area in western red cedar (Thuja plicata) seedlings. *Tree Physiology*, 22(6), 363– 371. https://doi.org/10.1093/treephys/22.6.363

Quero, J. L., Villar, R., Maranon, T., & Zamora, R. (2006). Interactions of drought and shade effects on seedlings of four Quercus species: Physiological and structural leaf responses. *New Phytologist*, 170(4), 819–834. https://doi.org/10.1111/j.1469-8137.2006.01713.x

Reichle, R. H., Draper, C. S., Liu, Q., Girotto, M., Mahanama, S. P. P., Koster, R. D., & De Lannoy, G. J. M. (2017). Assessment of MERRA-2 land surface hydrology estimates. *Journal of Climate*, 30(8), 2937– 2960. https://doi.org/10.1175/JCLI-D-16-0720.1

Reichle, R. H., Liu, Q., Koster, R. D., Draper, C. S., Mahanama, S. P. P., & Partyka, G. S. (2017). Land surface precipitation in MERRA-2. *Journal of Climate*, 30(5), 1643– 1664. https://doi.org/10.1175/JCLI-D-16-0570.1

Rienecker, M. M., Suarez, M. J., Gelaro, R., Todling, R., Bacmeister, J., Liu, E., et al. (2011). MERRA: NASA's Modern-Era Retrospective Analysis for Research and Applications. *Journal of Climate*, 24(14), 3624– 3648. https://doi.org/10.1175/JCLI-D-11-00015.1

Savage, J., & Vellend, M. (2015). Elevational shifts, biotic homogenization and time lags in vegetation change during 40 years of climate warming. *Ecography*, 38(6), 546– 555. https://doi.org/10.1111/ecog.01131

Schlesinger, W. H., & Jasechko, S. (2014). Transpiration in the global water cycle. *Agricultural and Forest Meteorology*, 189, 115– 117.

Sellers, P. J., Randall, D. A., Collatz, G. J., Berry, J. A., Field, C. B., Dazlich, D. A., et al. (1996). A revised land surface parameterization (SiB2) for atmospheric GCMs.1. Model formulation. *Journal of Climate*, 9(4), 676– 705. https://doi.org/10.1175/1520-0442(1996)009%3C0676:Arlspf%3E2.0.Co;2

Shi, X. Y., Mao, J. F., Thornton, P. E., & Huang, M. Y. (2013). Spatiotemporal patterns of evapotranspiration in response to multiple environmental factors simulated by the Community Land Model. *Environmental Research Letters*, 8(2). https://doi.org/10.1088/1748-9326/8/2/024012

Simmons, A. J., Berrisford, P., Dee, D. P., Hersbach, H., Hirahara, S., & Thepaut, J. N. (2017). A reassessment of temperature variations and trends from global reanalyses and monthly surface climatological datasets. *Quarterly Journal of the Royal Meteorological Society*, 143(702), 101– 119. https://doi.org/10.1002/qj.2949

Sitch, S., Huntingford, C., Gedney, N., Levy, P. E., Lomas, M., Piao, S. L., et al. (2008). Evaluation of the terrestrial carbon cycle, future plant geography and climate-carbon cycle feedbacks using five dynamic global vegetation models (DGVMs). *Global Change Biology*, 14(9), 2015– 2039. https://doi.org/10.1111/j.1365-2486.2008.01626.x

Slot, M., & Winter, K. (2016). The effects of rising temperature on the ecophysiology of tropical forest trees. In G Goldstein & L. S. Santiago (Eds.), *Tropical tree physiology: Adaptations and responses in a changing environment* (pp. 385– 412). Cham: Springer International Publishing.

Sofo, A., Dichio, B., Montanaro, G., & Xiloyannis, C. (2009). Shade effect on photosynthesis and photoinhibition in olive during drought and rewatering. *Agricultural Water Management*, 96(8), 1201– 1206. https://doi.org/10.1016/j.agwat.2009.03.004

Soliveres, S., Smit, C., & Maestre, F. T. (2015). Moving forward on facilitation research: Response to changing environments and effects on the diversity, functioning and evolution of plant communities. *Biological Reviews*, 90(1), 297– 313. https://doi.org/10.1111/brv.12110

Spayd, S. E., Tarara, J. M., Mee, D. L., & Ferguson, J. C. (2002). Separation of sunlight and temperature effects on the composition of *Vitis vinifera* cv. Merlot berries. *American Journal of Enology and Viticulture*, 53(3), 171– 182.

Ukkola, A. M., & Prentice, I. C. (2013). A worldwide analysis of trends in water-balance evapotranspiration. *Hydrology and Earth System Sciences*, 17(10), 4177– 4187. https://doi.org/10.5194/hess-17-4177-2013

Urban, J., Ingwers, M., McGuire, M. A., & Teskey, R. O. (2017a). Stomatal conductance increases with rising temperature. *Plant Signaling & Behavior*, 12(8), e1356534. https://doi.org/10.1080/15592324.2017.1356534

Urban, J., Ingwers, M. W., McGuire, M. A., & Teskey, R. O. (2017b). Increase in leaf temperature opens stomata and decouples net photosynthesis from stomatal conductance in Pinus taeda and *Populus deltoides* x nigra. *Journal of Experimental Botany*, 68(7), 1757– 1767. https://doi.org/10.1093/jxb/erx052

Valladares, F., Laanisto, L., Niinemets, U., & Zavala, M. A. (2016). Shedding light on shade: Ecological perspectives of understorey plant life. *Plant Ecology and Diversity*, 9(3), 237– 251. https://doi.org/10.1080/17550874.2016.1210262

Vazquez, D. P., Gianoli, E., Morris, W. F., & Bozinovic, F. (2017). Ecological and evolutionary impacts of changing climatic variability. *Biological Reviews*, 92(1), 22– 42. https://doi.org/10.1111/brv.12216

Wang, Q., Tenhunen, J., Falge, E., Bernhofer, C., Granier, A., & Vesala, T. (2004). Simulation and scaling of temporal variation in gross primary production for coniferous and deciduous temperate forests. *Global Change Biology*, 10(1), 37– 51. https://doi.org/10.1111/j.1365-2486.2003.00716.x

Wei, Z., Yoshimura, K., Wang, L., Miralles, D. G., Jasechko, S., & Lee, X. (2017). Revisiting the contribution of transpiration to global terrestrial evapotranspiration. *Geophysical Research Letters*, 44(6), 2792– 2801. https://doi.org/10.1002/2016GL072235

Williams, C. A. (2014). Heat and drought extremes likely to stress ecosystem productivity equally or more in a warmer, CO_2 rich future. *Environmental Research Letters*, 9(10), 101002. Retrieved from http://stacks.iop.org/1748-9326/9/i=10/a=101002

Wolz, K. J., Wertin, T. M., Abordo, M., Wang, D., & Leakey, A. D. B. (2017). Diversity in stomatal function is integral to modelling plant carbon and water fluxes. *Nature Ecology & Evolution*, 1(9), 1292– 1298. https://doi.org/10.1038/s41559-017-0238-z

Zeng, Z. Z., Piao, S. L., Lin, X., Yin, G. D., Peng, S. S., Ciais, P., & Myneni, R. B. (2012). Global evapotranspiration over the past three decades: Estimation based on the water balance equation combined with empirical models. *Environmental Research Letters*, 7(1). https://doi.org/10.1088/1748-9326/7/1/014026

Zeng, Z. Z., Wang, T., Zhou, F., Ciais, P., Mao, J. F., Shi, X. Y., & Piao, S. L. (2014). A worldwide analysis of spatiotemporal changes in water balance-based evapotranspiration from 1982 to 2009. *Journal of Geophysical Research: Atmospheres*, 119, 1186– 1202. https://doi.org/10.1002/2013JD020941

Zeng, Z. Z., Zhu, Z. C., Lian, X., Li, L. Z. X., Chen, A. P., He, X. G., & Piao, S. L. (2016). Responses of land evapotranspiration to Earth's greening in CMIP5 Earth System Models. *Environmental Research Letters*, 11(10). https://doi.org/10.1088/1748-9326/11/10/104006

Zhang, Y., Xiao, X. M., Wu, X. C., Zhou, S., Zhang, G. L., Qin, Y. W., & Dong, J. W. (2017). Data descriptor: A global moderate resolution dataset of gross primary production of vegetation for 2000-2016. *Scientific Data*, 4, 170165. https://doi.org/10.1038/sdata.2017.165

Zhang, Y., Xiao, X. M., Zhou, S., Ciais, P., McCarthy, H., & Luo, Y. Q. (2016). Canopy and physiological controls of GPP during drought and heat wave. *Geophysical Research Letters*, 43, 3325– 3333. https://doi.org/10.1002/2016GL068501

Zhang, Y. Q., Chiew, F. H. S., Pena-Arancibia, J., Sun, F. B., Li, H. X., & Leuning, R. (2017). Global variation of transpiration and soil evaporation and the role of their major climate drivers. *Journal of Geophysical Research: Atmospheres*, 122, 6868– 6881. https://doi.org/10.1002/2017JD027025

Zhang, Y., Peña-Arancibia, J. L., McVicar, T. R., Chiew, F. H. S., Vaze, J., Liu, C., et al. (2016). Multi-decadal trends in global terrestrial evapotranspiration and its components. *Scientific Reports*, 6, 19124. https://doi.org/10.1038/srep19124

Zhu, Z. C., Bi, J., Pan, Y. Z., Ganguly, S., Anav, A., Xu, L., et al. (2013). Global data sets of vegetation leaf area index (LAI)3g and fraction of photosynthetically active radiation (FPAR)3g derived from Global Inventory Modeling and Mapping Studies (GIMMS) normalized difference vegetation index (NDVI3g) for the period 1981 to 2011. *Remote Sensing*, 5(2), 927–948.

Zhu, Z. C., Piao, S. L., Myneni, R. B., Huang, M. T., Zeng, Z. Z., Canadell, J. G., et al. (2016). Greening of the Earth and its drivers. *Nature Climate Change*, 6(8), 791.